

CFD ANALYSIS ON AERODYNAMIC BEHAVIOUR OF NACA 0018 AND NACA 0012 AIRFOILS AT LOW REYNOLDS NUMBER

Abdus Shabur¹, Asif Hasan Khan² and Mohammad Ali³

¹Dept. of Mechatronics and Industrial Engineering, CUET, Bangladesh

²Dasherbandi Sewage Treatment Plant (500MLD) Project, Bangladesh

³Dept. of Mechanical Engineering, BUET, Bangladesh

abdusshabur@cuet.ac.bd*, asif.ananta2013@gmail.com, mali@me.buet.ac.bd

Abstract- For better designing of an airfoil, the aerodynamic characteristics of the airfoil need to be investigated both experimentally and numerically. Coefficient of lift (C_L), coefficient of drag (C_D), variation of C_L/C_D ratio with angle of attack are very important parameters in CFD analysis. In this study the above parameters are investigated for two symmetric airfoils (NACA0018 and NACA0012) at two different low Reynolds numbers of 300,000 and 700,000. This numerical results show that the stall angle for NACA0018 airfoil at $Re=300,000$ is less than 17 degree and at $Re=700,000$ for the same airfoil it is 17.5 degree and this happened due to the increased velocity. C_L increases more linearly than C_D up to about 10 degree so that C_L/C_D ratio increases with the angle of attack and then decreases after or near about 10 degree. It has been also found that higher the Reynolds number, greater the value of C_L/C_D ratio. Besides, it is evident from this simulation that NACA 0012 produces more lift than NACA 0018 for the same Reynolds number. That's why, NACA 0012 airfoil may be verily used for aircraft application whereas NACA 0018 airfoil may be used in VAWT (Vertical Axis Wind Turbine) And HAWT (Horizontal Axis Wind Turbine) to capture the wind energy and convert it to useable energy which is one form of renewable energy.

Keywords: Airfoil, Reynolds number, NACA, Angle of Attack, Velocity

1. INTRODUCTION

The aerodynamic characteristics of any airfoil need to be analyzed and that's why different parameters associated with aerodynamics are must to be investigated both experimentally and numerically for required performance of airfoil. An airfoil is the cross-sectional shape of a wing, blade (of a propeller, rotor, or turbine), or sail. An airfoil-shaped body moved through a fluid produces an aerodynamic force. The component of this force perpendicular to the direction of motion is called lift. The component parallel to the direction of motion is called drag. Subsonic flight airfoils have a characteristic shape with a rounded leading edge, followed by a sharp trailing edge, often with a symmetric curvature of upper and lower surfaces. Foils of similar function designed with water as the working fluid are called hydrofoils. Coefficient of lift (C_L), coefficient of drag (C_D), variation of C_L/C_D ratio with angle of attack are important parameters in Computational Fluid Dynamics (CFD) analysis. Various modeling like Standard k- ϵ , RNG k- ϵ , SST k- ω etc. are frequently used to determine these parameters of an airfoil, both symmetric and asymmetric. In this study the above parameters are investigated for two symmetric airfoils (NACA0018 and NACA0012) at two different low Reynolds numbers of 300,000 and 700,000. NACA stands for National Advisory Committee for Aeronautics. A commercial CFD code, the FLUENT (version 14.5), is used in this study. SST k- ω turbulence model is used for calculating C_L , C_D variation with angle of attack. We have validated our

numerical simulation with a known experimental investigation.

2. LITERATURE REVIEW

Sereez et al. [2] analyzed aerodynamic static hysteresis at stall conditions for NACA0018 airfoil in the TsAGI's T-124 low-turbulence wind tunnel. Comparisons of computational simulation results with experimental wind tunnel data were made for 2D NACA0018 and NACA0012 airfoils at low Reynolds numbers $Re = 300,000$. The study showed the width of static hysteresis loop was different in static tests and during slow sweep variation of angle of attack indicating sensitivity of abrupt transitions between different separated flow structures.

Jacobs and Sherman [10] investigated symmetric airfoil in NACA variable-density wind tunnel over a wide range of Reynolds number extending well into the flight range. The tests were made to provide information from which the variations of airfoil section characteristics with changes in the Reynolds number could be inferred and methods of allowing for these variations in practice could be determined.

Timmer [11] performed balance and wake rake measurements on a 0.25 m chord model having a NACA 0018 airfoil in the Delft University low-turbulence wind tunnel. The test showed that lower surface laminar separation bubble dominates the flow and noise characteristics at Reynolds numbers between 150000 and 1000000. This study gave the experimental data for C_D vs. angle of attack and C_L vs. angle of attack.

3. NUMERICAL APPROACH

3.1 Basics of CFD

Computational fluid dynamics constitutes a relatively new approach in the philosophical study and development of the whole discipline of fluid dynamics. The innovation of the high speed digital computer combined with the development of accurate numerical algorithms for solving physical problems on these computers has revolutionized the way we practice fluid dynamics today. Computational fluid dynamics is today an equal partner with pure theory and pure experiment in the analysis and solution of fluid dynamics problems. Applying the fundamental laws of mechanics to a fluid gives the governing equations for a fluid.

3.1 Governing Equation

The conservation of mass equation is in vector form

$$\frac{\partial \rho}{\partial t} + \nabla \cdot (\rho V) = 0 \quad (1)$$

And the conservation of momentum equation is

$$\rho \frac{\partial V}{\partial t} + \rho((V \cdot) V) = -\nabla p + \rho g + \nabla \cdot \tau \quad (2)$$

Where, ∇ is the velocity vector.

The governing equation for the present study is the Continuity Equation (Conservation of Mass) and Navier-Stokes Equation (Conservation of Momentum) for incompressible (density, ρ is constant) flow.

1. Conservation of mass

$$\frac{1}{\rho} \frac{\partial \rho}{\partial t} + \frac{\partial(u)}{\partial x} + \frac{\partial(v)}{\partial y} + \frac{\partial(w)}{\partial z} = 0 \quad ; \text{For 3D flow} \quad (3)$$

$$\frac{1}{\rho} \frac{\partial \rho}{\partial t} + \frac{\partial(u)}{\partial x} + \frac{\partial(v)}{\partial y} = 0 \quad ; \text{For 2D flow} \quad (4)$$

2. Conservation of momentum

For 3-D flow,

$$\rho \left(\frac{\partial(u)}{\partial t} + u \frac{\partial(u)}{\partial x} + v \frac{\partial(u)}{\partial y} + w \frac{\partial(u)}{\partial z} \right) + \frac{\partial(\rho)}{\partial x} = \mu \left(\frac{\partial^2(u)}{\partial x^2} + \frac{\partial^2(u)}{\partial y^2} + \frac{\partial^2(u)}{\partial z^2} \right) \quad (5)$$

$$\rho \left(\frac{\partial(v)}{\partial t} + u \frac{\partial(v)}{\partial x} + v \frac{\partial(v)}{\partial y} + w \frac{\partial(v)}{\partial z} \right) + \frac{\partial(\rho)}{\partial y} = \mu \left(\frac{\partial^2(v)}{\partial x^2} + \frac{\partial^2(v)}{\partial y^2} + \frac{\partial^2(v)}{\partial z^2} \right) \quad (6)$$

$$\rho \left(\frac{\partial(w)}{\partial t} + u \frac{\partial(w)}{\partial x} + v \frac{\partial(w)}{\partial y} + w \frac{\partial(w)}{\partial z} \right) + \frac{\partial(\rho)}{\partial z} = \mu \left(\frac{\partial^2(w)}{\partial x^2} + \frac{\partial^2(w)}{\partial y^2} + \frac{\partial^2(w)}{\partial z^2} \right) \quad (7)$$

3.2 Geometry

Figure 1 and Figure 2 depict the airfoil used in present study. The chord length is 1m for both airfoils. The radius of the 'C' of the C-shaped mesh is 12.5m. The maximum thickness for NACA0012 airfoil is 12% of the chord length and for NACA0018 it is 18% of the chord length.



Fig.1: NACA 0012 airfoil



Fig.2: NACA 0018 airfoil

3.3 Meshing

Grid system is very important for quality CFD analysis. In the present study, a 2D unstructured mesh is employed with total number of cells about 89000 in both airfoils. The maximum and minimum face area is 2.323256 m^2 and $2.011792 \times 10^{-4} \text{ m}^2$ respectively for NACA 0012 airfoil which is 3.360926 m^2 and $1.896361 \times 10^{-4} \text{ m}^2$ respectively for NACA 0018 airfoil. The meshing domain is shown in Figure 3. Zoomed in views of the meshing near the airfoil surfaces are given in Figure 4.

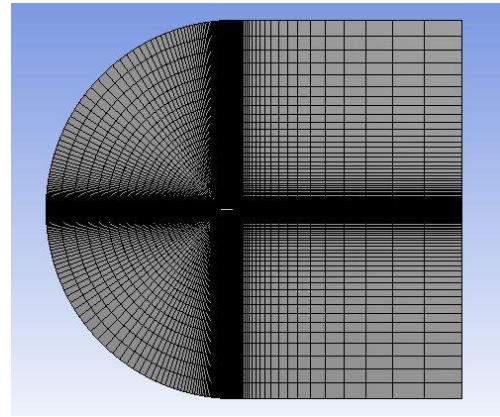


Fig.3: Meshing domain for NACA 0018 airfoil

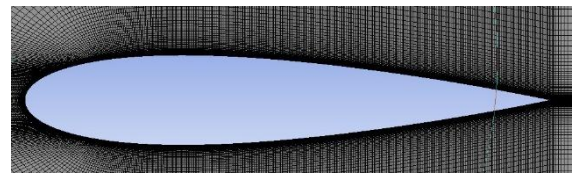


Fig.4: Magnified view of meshing for NACA0018 airfoil

3.4 Solver Setting

ANSYS FLUENT is used for computation. SST k- ω turbulence model is used for calculating C_L , C_D variation with angle of. This CFD tool solved the governing integral equations for the conservation of mass and momentum.

Table 1: Solver Setting

Solver	Velocity formulation	2D Space	Time
Pressure based	Absolute	Planer	Steady

3.5 Boundary Conditions

Inlet: Velocity inlet boundary condition is used. For $Re=300,000$ the inlet velocity was used 4.38 m/s and for $Re=700,000$ the inlet velocity was 10.23 m/s.

Outlet: Pressure outlet boundary condition is used. At the outlet boundary, gauge pressure is maintained as 0 Pa.

Wall: At all solid boundaries in the flow geometry stationary wall with the no-slip condition has been used. It can be mathematically expressed as,
 $u_{wall}=0$ m/s, and $v_{wall}=0$ m/s

3.6 Solution Method

In this study Coupled scheme was used for pressure-velocity coupling. This solver offers some advantages over the pressure-based segregated algorithm. The pressure-based coupled algorithm obtains a more robust and efficient single phase implementation for steady-state flows. In the spatial discretization gradient was least squares cell based, Pressure was second order, momentum was second order upwind, turbulent kinetic energy and specific dissipation rate were used as first order upwind. Courant-Friedrichs-Lewy (CFL) number was kept 0.9 and explicit relaxation factors for pressure and momentum were both 0.75.

4. RESULTS AND DISCUSSION

4.1 Validation

For validation here we have used two experimental investigation. One is Jacobs [10] in 1937 and another is Timmer [11] in 2008. Our calculated results have nearly matched with these both experimental results. We have validated our results for NACA0018 airfoil differently at $Re=300000$ and $Re=700000$. The graphical results of validation is shown below:

Table 2 Comparison between C_L and C_D of our models and the available experimental data for NACA 0018 at $Re = 300,000$

C_L			
AOA	Our Study	Jacob	Timmer
5°	0.43726	0.48	0.47
10°	0.85221	0.85	0.93
15°	1.2207	1.00	1.04

C_D			
AOA	Our Study	Jacob	Timmer
5°	0.017397	0.024	.023
10°	0.025715	0.028	0.027
15°	0.051888	0.04	0.06

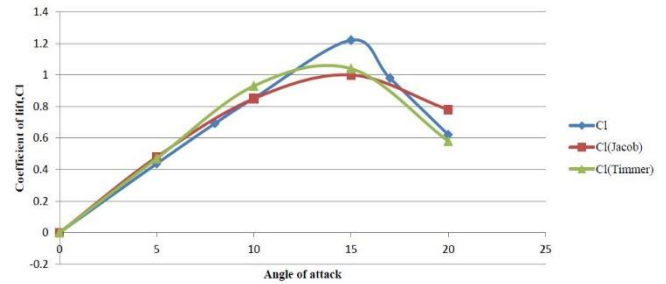


Fig.5: Comparison between the calculated coefficient of lift (C_L) of our models and the available experimental data for NACA 0018 at $Re = 300,000$

From Figure 5, it is evident that the C_L is proportional with angle of attack up to the stall angle (which is almost 16 degree) and beyond that angle C_L suddenly falls. This is due to back flow of the air stream.

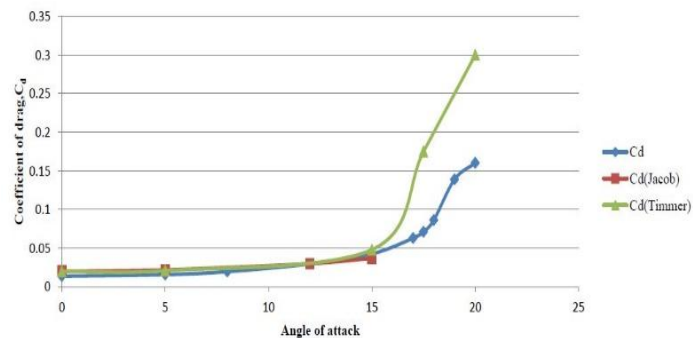


Fig.6: Comparison between the calculated coefficient of drag (C_D) of our models and the available experimental data for NACA 0018 at $Re = 700,000$

From these graphs, it can be said that our simulation work is valid. Up to stall angle our studied data almost matches with the experimental data, but after the stall angle the characteristics is unpredictable.

4.2 Results

4.2.1 Effect of the Shape (Maximum Thickness) of the Airfoil on C_L/C_D ratio

We know the thrust is a very important parameter for flying of airplane. The thrust required for an airplane to fly at a given velocity in steady level flight is

$$TR = \frac{W}{C_L/C_D} \quad (8)$$

Where TR is Thrust Required and W is Weight of the airplane. Here from Equation 8, we see that thrust required is inversely proportional with C_L/C_D ratio. Higher the value of C_L/C_D ratio, lower the amount of thrust required. That's why, in aerodynamics of airplane it is often desired to maximize the C_L/C_D ratio.

In our study, it has been noticed the variation C_L/C_D ratio with angle of attack for both airfoils at different Reynold's numbers and found an interesting result.

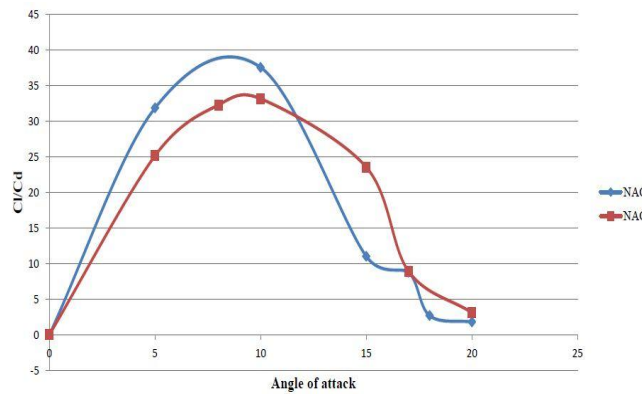


Fig.7: Variation of C_L/C_D ratio with angle of attack for NACA0018 and NACA0012 at $Re=300,000$

From Figure 7, it is evident that the maximum value of C_L/C_D ratio is higher for NACA0012 over NACA0018 for same Reynolds number (300,000). The cause of this phenomena may be the thickness of the airfoil. As the thickness of NACA0012 is lower than the NACA0018, so it faces comparatively less frictional drag. As a consequence, the C_L/C_D ratio slightly increases. After the peak point the C_L/C_D ratio decreases rapidly in case of NACA0012 airfoil while the ratio decreases slowly for NACA0018 airfoil.

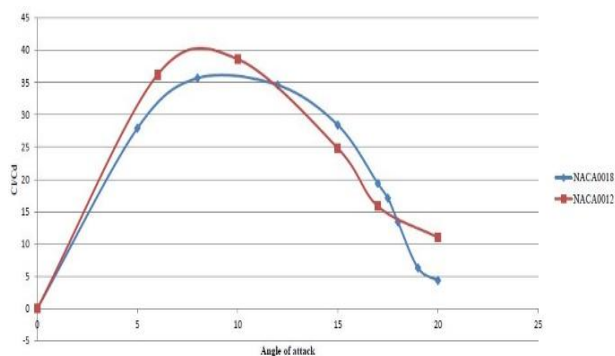


Fig.8: Variation of C_L/C_D ratio with angle of attack for NACA0018 and NACA0012 at $Re=700,000$

In Figure 8, the variation has been illustrated for $Re=700,000$. Here it is seen that the maximum value of the ratio is slightly higher than for $Re=300,000$. This phenomena is due to the increase in Reynolds number i.e. velocity. The maximum ratio is compared in the following table:

Table: 3 Comparison of maximum C_L/C_D with $Re=300,000$ and $Re=700,000$

Airfoil	$Re=300,000$	$Re=700,000$
NACA0012	38.023	40.056
NACA0018	33.89	36.42

From the above comparison, it is clear that the maximum C_L/C_D ratio is always greater for NACA0012 airfoil than

NACA0018 airfoil. For this reason NACA0012 airfoil is extensively used in aircraft where Lift is of prime concern and on the contrary NACA0018 airfoil is used in the vertical axis wind turbine blades and other cases where lift is not of prime interest.

4.2.2 Effect of Reynolds Number (Free-Stream Velocity) on the C_L/C_D Ratio

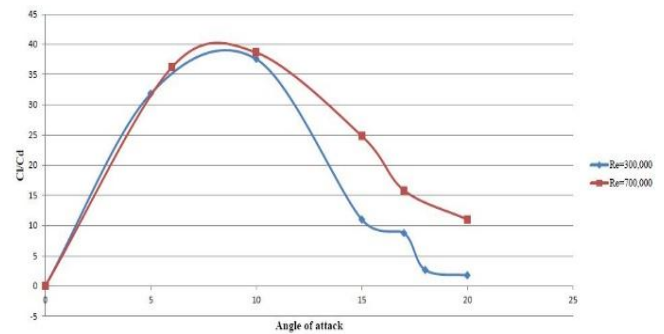


Fig.9: Variation of C_L/C_D ratio with angle of attack for NACA0012 at $Re=300,000$ and $Re=700,000$

From Figure 9, it is seen that up to about 5 degree of angle of attack, the C_L/C_D ratio is slightly higher for $Re=300,000$ but the maximum value of the ratio is higher for $Re=700,000$. After the peak point the ratio decreases rapidly for $Re=300,000$. This happens because for lower Reynolds number as the velocity is lower and the flow tends to be attached to the surface and therefore, drag increased and overall C_L/C_D ratio is decreased more.

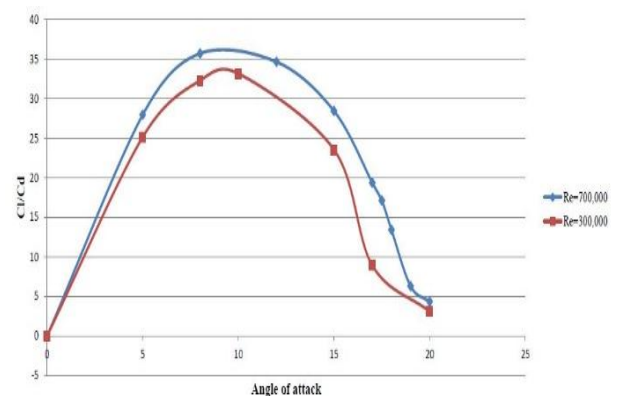


Fig.10: Variation of C_L/C_D with angle of attack for NACA0018 at $Re=300,000$ and $Re=700,000$

From the Figure 10, it is seen that the C_L/C_D ratio is always lower unlike for the NACA0012 airfoil where initially the ratio is slightly higher for $Re=300,000$

5. CONCLUSION

In this study, we have tried to find some aerodynamic properties and finally found that C_L/C_D ratio is always higher for NACA 0012 than NACA 0018 airfoil. At the same time, with the increase of Reynold's number, C_L/C_D ratio increases for both airfoils. We have also seen that C_L/C_D ratio increases almost linearly with the angle of

attack. But after a certain angle of attack, the C_L/C_D ratio abruptly falls down. So this angle is very crucial for aerodynamics. It is evident from our simulation that NACA 0012 produces more lift than NACA 0018 for the same Reynolds number. That's why, NACA 0012 airfoil may be verily used for aircraft application whereas NACA 0018 airfoil may be used in VAWT (Vertical Axis Wind Turbine) And HAWT (Horizontal Axis Wind Turbine) to capture the wind energy as a form of wind turbine blade and convert it to useable energy which is one form of renewable energy.

6. ACKNOWLEDGEMENT

At first we want to express gratitude to almighty Allah for giving us the strength to complete our work. We would like to express our deepest gratitude to the all teachers of Department of Mechanical Engineering, BUET for their valuable guidance and suggestion throughout this study. Without their initiative ideas, talents, guidelines and encouragements, this work would not have been possible to complete successfully. Higher Education Quality Enhancement Project (HEQEP), UGC, MoE, GoB provided us the opportunity to use high speed computational facilities. So we are really grateful to HEQEP (CP#2099- Development of Research Facilities on Biomedical Fluid Flow Phenomena) for providing us with AeroLab and computational resources.

7. NOMENCLATURE

Symbol	Meaning	Unit
α	Angle of attack	(K)
P	Pressure	(Pa)
c	Chord length	(m)
x	Any distance from leading edge	(m)
u	X-component velocity	(m/s)
v	Y-component velocity	(m/s)
w	Z-component velocity	(m/s)
V_∞	Free-stream velocity	(m/s)
τ	Shear stress	(N/m ²)
μ	Viscosity	(Pa-s)
ρ	Density	(kg/m ³)
Re	Reynolds number ($\rho V_\infty L / \mu$)	Dimens ion Less
t	Time	(s)
C_L	Coefficient of lift	Dimens ion Less
C_D	Coefficient of drag	Dimens ion Less

8. REFERENCES

- [1] Hassan, G. E., Hassan, A., & Youssef, M. E. (2015).
- [2] Numerical investigation of medium range re numbers aerodynamics characteristics for NACA0018 airfoil. CFD letters, 6(4), 175-187.
- [3] Sereez, M., Abramov, N., & Goman, M. (2016, July). Computational Simulation of Airfoils Stall Aerodynamics at Low Reynolds Numbers. Royal Aeronautical Society, Applied Aerodynamics Conference.
- [4] Ladson, C. L. (1988). Effects of independent variation of Mach and Reynolds numbers on the low-speed aerodynamic characteristics of the NACA 0012 airfoil section.
- [5] Brendel, M. (1987). Experimental Study Of The Boundary Layer On A Low Reynolds Number Airfoil In Steady And Unsteady Flow.
- [6] Abbott, I. H., & Von Doenhoff, A. E. (1959). Theory of wing sections, including a summary of airfoil data. Courier Corporation.
- [7] www.naca.com
- [8] Brendel, M., & Mueller, T. J. (1988). Boundary-layer measurements on an airfoil at low Reynolds numbers. Journal of aircraft, 25(7), 612-617.
- [9] Hu, H., Yang, Z., & Igarashi, H. (2007). Aerodynamic hysteresis of a low-Reynolds-number airfoil. Journal of Aircraft, 44(6), 2083-2086.
- [10] Jacobs, E. N., & Sherman, A. (1937). Airfoil section characteristics as affected by variations of the Reynolds number.
- [11] Timmer, W. A. (2008). Two-dimensional low-Reynolds number wind tunnel results for airfoil NACA 0018. Wind engineering, 32(6), 525-537.
- [12] Anderson Jr, J. D. (2010). Fundamentals of aerodynamics. Tata McGraw-Hill Education.
- [13] Release, A. N. S. Y. S. (2012). 14.5, User Guide. ANSYS, Inc.